Aerosol-assisted CVD of bismuth vanadate thin films and their photoelectrochemical properties

Chemical Vapor Deposition

DOI: 10.1002/cvde.201407142

Full Paper

Aerosol-Assisted CVD of Bismuth Vanadate Thin Films and Their Photoelectrochemical Properties**

By *Paul Brack, Jagdeep S. Sagu, T. A. Nirmal Peiris, Andrew McInnes, Mauro Senili, K. G. Upul Wijayantha*, Frank Marken,* and *Elena Selli*

Thin film bismuth vanadate ($BiVO_4$) photoelectrodes are prepared by aerosol-assisted (AA)CVD for the first time on fluorine-doped tin oxide (FTO) glass substrates. The $BiVO_4$ photoelectrodes are characterised by X-ray diffraction (XRD), Raman spectroscopy (RS), and energy-dispersive X-ray (EDX) spectroscopy and are found to consist of phase-pure monoclinic $BiVO_4$. Scanning electron microscopy (SEM) analysis shows that the thin film is uniform with a porous structure, and consists of particles approximately 75–125 nm in diameter. The photoelectrochemical (PEC) properties of the $BiVO_4$ photoelectrodes are studied in aqueous 1 M Na_2SO_4 and show photocurrent densities of 0.4 mA cm^{-2}, and a maximum incident-photon-to-electron conversion efficiency (IPCE) of 19% at 1.23 V vs. the reversible hydrogen electrode (RHE). $BiVO_4$ photoelectrodes prepared by this method are thus highly promising for use in PEC water-splitting cells.

Keywords: AACVD, $BiVO_4$, Photoelectrochemical, Thin film, Water splitting

1. Introduction

The need for renewable, non-polluting sources of energy is acute. One such energy source is the sun. There are many successful systems currently available which can transform solar energy to electrical energy. A key issue which must be addressed in harvesting and utilising solar energy is the storage of electrical energy. It is thus preferable to transform solar energy directly into the more easily stored and transported form of chemical energy through the formation of chemical bonds in molecules such as hydrogen.

One way to achieve this is to use PEC cells.[1–4] These consist of electrodes made of light-absorbing semiconductors dipped into an electrolytic solution, and use sunlight to split water into oxygen (at the anode) and hydrogen (at the cathode) as described by Equation 1 and 2, respectively (under acidic conditions).[1]

$$H_2O + 2\ h^+ \rightarrow 1/2\ O_2 + 2\ H^+ \quad (1)$$

$$2\ H^+ + 2\ e^- \rightarrow H_2 \quad (2)$$

$BiVO_4$ has risen to prominence of late as one of the most promising anodic semiconductor materials for use in PEC cells. The PEC properties of $BiVO_4$ are dependent upon its band energetics and are determined by key parameters such as its crystal structure (bulk) and surface properties. The best PEC properties are exhibited by $BiVO_4$ in the monoclinic scheelite crystal structure, which has a band gap of 2.4 eV.[5] Although this is slightly larger than the projected ideal band gap for a photoanode (typically around 2 eV), this minor disadvantage is more than counteracted by the position of its band edges. The conduction band edge (0 V vs. the normal hydrogen electrode (NHE) at pH 0) is almost sufficiently negative with respect to the hydrogen evolution potential, whilst the valence band edge (2.4 V vs. NHE at pH 0) is suitably placed to allow water oxidation.[6,7] In addition, $BiVO_4$ is one of the few photoanodic materials which are stable in mild, pH neutral conditions.[8]

This interest in $BiVO_4$ has led to a considerable amount of recent work on the preparation of nanostructured $BiVO_4$ films by low-cost and scalable methods which include spray pyrolysis, CVD, electrodeposition, dip coating, and seed layer mediated growth.[9–16] Many published methods to date, however, produce films which are poorly adhered to

[*] P. Brack, J. S. Sagu, Dr. T. A. N. Peiris, A. McInnes, Prof. K. G. U. Wijayantha
Department of Chemistry, Energy Research Laboratory, Loughborough University, Loughborough LE11 3TU, United Kingdom
E-mail: U.Wijayantha@lboro.ac.uk
M. Senili, Prof. E. Selli
Department of Chemistry, University of Milan, Milano 20133, Italy
Prof. F. Marken
Department of Chemistry, University of Bath, Bath BA2 7AY, United Kingdom

[**] Authors acknowledge the support received from UK ESPRC through the Doctoral Training Centre for Hydrogen, Fuel cells and their applications. The work was also supported by Loughborough University. Authors also acknowledge the assistance given by the members of Energy Research Laboratory in the Department of Chemistry, Loughborough University.

the substrate or have large particle sizes, neither of which is ideal for PEC processes, or require multiple synthetic steps to produce the electrodes. We have previously reported on the one-step fabrication of highly efficient nanostructured thin film photoelectrode materials by the simple, low-cost, and readily scalable method of AACVD.[17–23] AACVD has several advantages over conventional CVD techniques.[24,25] It allows the use of non-volatile and thermally unstable precursors, better control of deposit stoichiometry, a higher rate of deposition, and a more flexible reaction environment than CVD (as it can be operated under atmospheric pressure in an open system). Several examples of the deposition of other bismuth-containing films by AACVD can be found in the literature.[26–29] Herein we report the extension of this methodology to the deposition of high-performance nanostructured $BiVO_4$ thin film photoelectrodes.

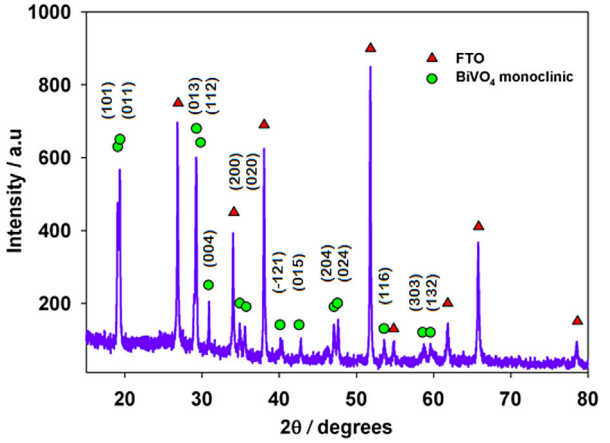

Fig. 1. XRD pattern of a $BiVO_4$ thin film fabricated by AACVD on a FTO glass substrate. The reflections due to the FTO substrate are denoted by the red triangles, and the reflections arising from the monoclinic $BiVO_4$ phase are denoted by the green circles.

2. Results and Discussion

2.1. Materials Characterisation

In its natural mineral form (pucherite), $BiVO_4$ exists in an orthorhombic crystal structure. Laboratory preparations of $BiVO_4$, however, crystallise in either a monoclinic or tetragonal scheelite (band gap 2.4 eV) or a tetragonal zircon-type structure (band gap 2.9 eV).[6] The smaller size of its band gap is what gives scheelite $BiVO_4$ improved photocatalytic properties compared to zircon-type $BiVO_4$. The difference in band gap arises from differences in the electronic band structure of $BiVO_4$ in the two forms. Specifically, in the scheelite structure, the 6 s orbital of Bi^{3+} is at higher energy than the O 2p orbital, allowing lower energy transitions to the V 3 d orbital and narrowing the band gap compared to the zircon-type structure, where the Bi^{3+} 6s orbital is at lower energy than the O 2p orbital and the photoinduced electronic transitions are thus of higher energy and widen the band gap.[30]

Although the monoclinic and tetragonal scheelite forms of $BiVO_4$ have the same band gap energy, the monoclinic form is found to have superior PEC performance. This has been ascribed to a greater distortion in the local environment of Bi^{3+} in the monoclinic structure causing increased local polarisation which eases electron-hole separation and thus enhances the photocatalytic properties.[31] Hence it is desirable that $BiVO_4$ thin films for PEC applications be formed in the monoclinic scheelite crystal structure.

Interestingly, XRD analysis confirmed that this was indeed the case for the films made by AACVD in the present work. In Figure 1, the peaks indicated by a red triangle correspond to the FTO glass substrate. The other two prominent peaks correspond to the (011) and (112) reflections of monoclinic scheelite $BiVO_4$ (PDF 01–075-1866), with shoulders corresponding to the (101) and (013) reflections. Notably, the (011) and (112) reflections are of higher relative intensity than in the database pattern, showing that the films have a preferred orientation in the direction of these planes. The presence of minor peaks such as (004), (200), (020), (015), (204), (024), (116), (303), and (132) further confirms the presence of monoclinic $BiVO_4$. The films are highly crystalline and free from any other phases of $BiVO_4$.

The Raman spectrum shown in Figure 2 further confirms the formation of monoclinic scheelite $BiVO_4$. The strongest peak at 827 cm^{-1} corresponds to antisymmetric stretching modes of the VO_4 tetrahedra, whilst the shoulder peak at 718 cm^{-1} is attributed to symmetric stretching modes of the same. The peaks at 366 and 326 cm^{-1} are due to the bending modes of the VO_4 tetrahedra, and the peaks at 211 and 129 cm^{-1} correspond to the vibration of the crystal lattice (external modes). The peaks in the spectrum show good

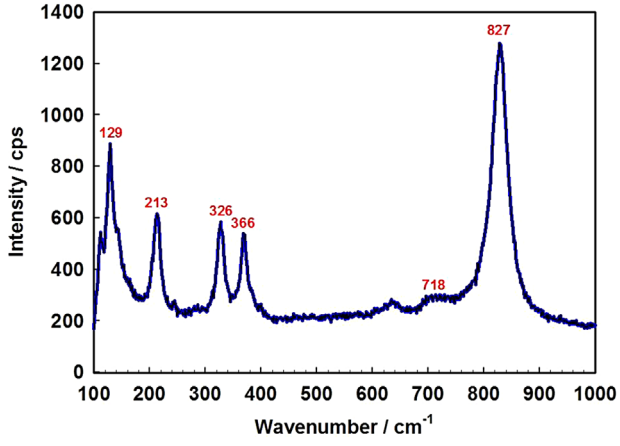

Fig. 2. Raman spectrum of a $BiVO_4$ thin film fabricated by AACVD on a FTO glass substrate.

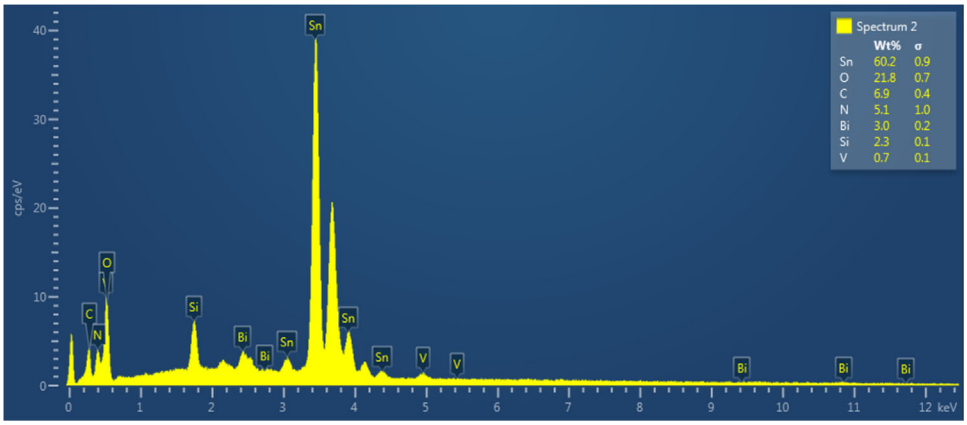

Fig. 3. EDX spectrum of a $BiVO_4$ thin film fabricated by AACVD on a FTO glass substrate.

agreement with those previously reported for monoclinc scheelite $BiVO_4$.[32–34]

EDX analysis (Fig. 3) further confirmed the presence of $BiVO_4$. The Bi/V ratio was found to be 1.05:1, which shows that the Bi and V have been deposited by AACVD in the correct stoichiometry. Combustion of the solvent during the preparation of the electrode by AACVD is most likely the origin of the carbon observed in the EDX spectrum. The nanostructured $BiVO_4$ films deposited by AACVD were translucent and yellow in colour (Fig. 4).

The band gap of a direct band gap semiconductor material such as $BiVO_4$ can be estimated by use of a Tauc plot, where the extrapolation to the x-axis (i.e., where $(\alpha h\nu)^2 = 0$) of the linear region of a plot of $(\alpha h\nu)^2$ vs. electron energy in eV (α is the absorption coefficient of the material and $h\nu$ the energy of light) gives the direct band gap of the material.[5] The optical band gap (E_g) of the film was estimated by this method to be 2.44 eV (Fig. 4), which is in reasonable agreement with the value of 2.4 eV reported in the literature for monoclinic scheelite $BiVO_4$.[6]

The volume average mean crystalline size was deduced from the XRD by application of the Scherrer equation and found to be 76 nm, which is in reasonable agreement with the average particle diameter observed in SEM images (Fig. 5), showing that the films are relatively porous and made up of irregularly shaped particles approximately 75–125 nm in diameter. This porosity gives the films a large effective surface area and an increased electrode/

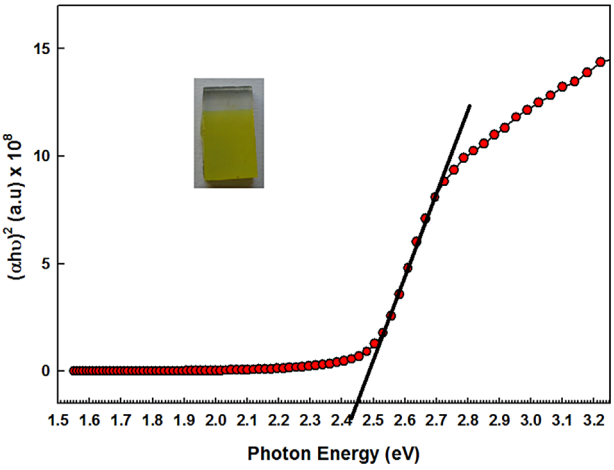

Fig. 4. A Tauc plot for a $BiVO_4$ thin film fabricated by AACVD. The band gap of the material is estimated from this plot to be 2.44 eV. The inset shows an image of a typical $BiVO_4$ thin film electrode prepared on a FTO glass substrate by AACVD. The adherence of the film was found to be excellent by the Scotch tape test.

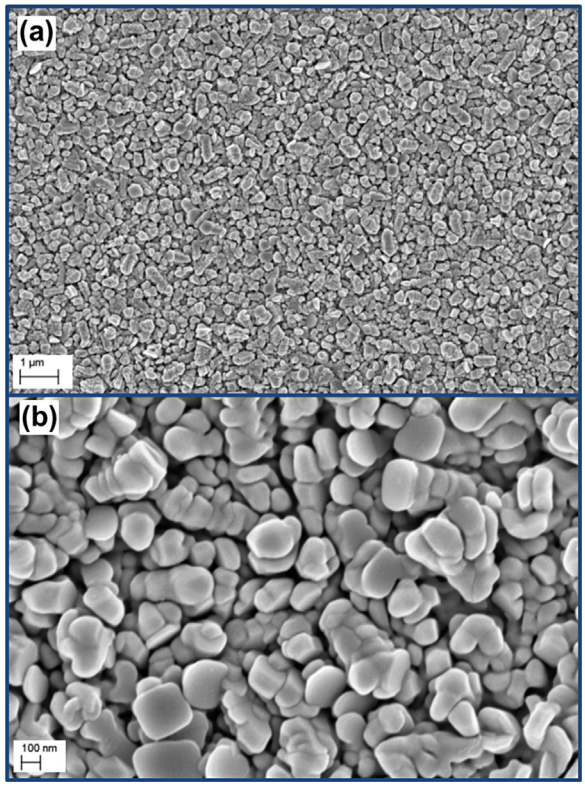

Fig. 5. SEM image of a $BiVO_4$ thin film at a magnification of a) 20 000 X and b) 100 000 X.

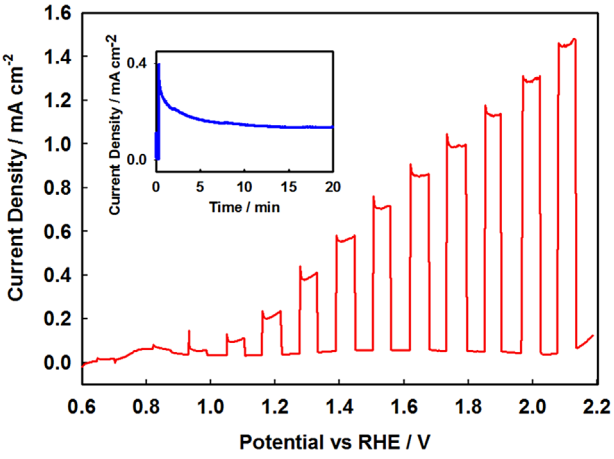

Fig. 6. *J-V* characteristics of a $BiVO_4$ thin film under chopped AM 1.5 100 mW cm^{-2} illumination measured in a three-electrode configuration, with an Ag/AgCl reference electrode and a platinum wire counter-electrode in 1.0 M Na_2SO_4. The inset shows the steady-state photocurrent stability measurement of the $BiVO_4$ photoanode in 1.0 M Na_2SO_4 at 1.23 V vs. RHE for 20 min.

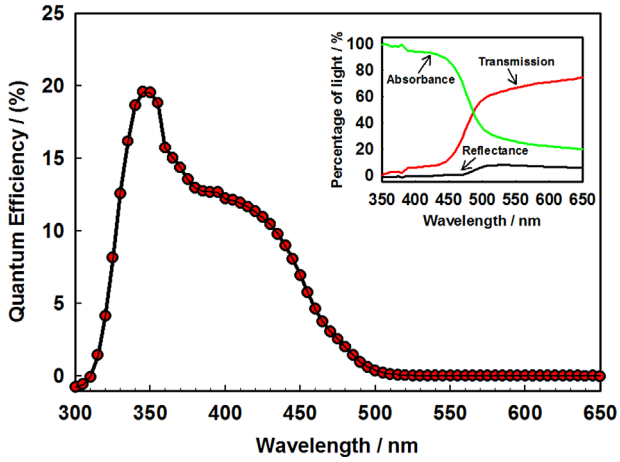

Fig. 7. IPCE spectrum for a $BiVO_4$ thin film measured in a three-electrode configuration, using a platinum wire counter-electrode and an Ag/AgCl reference electrode in a 1.0 M Na_2SO_4 electrolyte at 1.23 V vs. RHE. The inset shows the absorbance, transmission, and reflectance spectra for a $BiVO_4$ thin film synthesised by AACVD.

electrolyte interfacial area, leading to a reduction in electron-hole recombination as the photogenerated hole travels through less material before being collected at the electrode/electrolyte interface. The diameter of the particles matches well with the hole diffusion length of ~70 nm recently estimated for $BiVO_4$ films.[35] It is well known that hole collection can be improved for electrodes in which the feature size is comparable to the hole-diffusion length, and hence recombination is reduced, compared to films with larger features, and the PEC efficiency of the cell is increased.[15]

2.2. PEC Characterisation

PEC experiments were performed in 1.0 M Na_2SO_4 (pH 5.70) electrolyte by illuminating the $BiVO_4$ electrode from the substrate side with AM 1.5 simulated light. The photocurrent observed in this electrolyte corresponds to water oxidation. Experiments were conducted in both aerated and nitrogen-purged solutions, and there was no difference in the measured photocurrents, demonstrating that the oxygen produced by water oxidation has no effect on the continuing water-splitting process. Measurements were also carried out with electrolyte side illumination, but these showed consistently lower photocurrents than substrate side illumination, in line with what has previously been reported in the literature.[9,36,37] This suggests that either holes diffuse more easily than electrons in these films, or there is strong surface recombination due to the high surface-area to volume ratio of these films. Further work is currently underway in our laboratory to understand and distinguish these effects. Photocurrent density (J) was plotted against the applied bias potential, which was corrected for solution pH and reported vs. RHE.

1.23 V vs. RHE is the thermodynamic potential at which water oxidation (the anodic reaction in a PEC cell) occurs, and thus the photocurrent generated at this potential is commonly used as a standard for the comparison of different photoanodic materials. A photocurrent density of 0.4 mA cm^{-2} was obtained at 1.23 V vs. RHE for water oxidation, which compares favourably with values previously reported for unmodified bismuth vanadate films,[12,38] with a photocurrent onset of ~0.6 V vs. RHE. As shown in Figure 6, the observed photocurrent was found to decrease as the electrode was illuminated at 1.23 V vs. RHE. This phenomenon has been observed in bismuth vanadate photoanodes synthesised by other methods and is ascribed to photocorrosion of the electrode, though the exact mechanism is currently unknown.[9,16,39,40]

IPCE was calculated using the equation $IPCE = (1240 j_{ph}/\lambda I) \times 100\%$, where j_{ph} is the steady state photocurrent density [$\mu A\ cm^{-2}$], λ is the wavelength of the incident light [nm], and I is the light intensity at the surface of the film [$W\ m^{-2}$].[41] A maximum IPCE of 19% was observed at 355 nm at 1.23 V vs. RHE in 1.0 M Na_2SO_4, somewhat higher than many of the reported values for an unmodified bismuth vanadate thin film photoanode,[5,9] but rather lower than the best reported value of 73%.[42] IPCE rapidly decreased between 440 and 500 nm before dropping to zero at longer wavelengths, which is consistent with the absorption spectrum in Figure 7, and this behaviour is similar to that of $BiVO_4$ electrodes prepared by other methods.[43,44]

3. Conclusions

Herein we have presented the first report of the synthesis of $BiVO_4$ thin film photoelectrodes by a simple, low-cost,

and scalable AACVD method. These $BiVO_4$ electrodes show photocurrent densities as high as $0.4\,mA\,cm^{-2}$ at 1.23 V vs. RHE for water oxidation, and a maximum IPCE of 19% at 355 nm in 1.0 M Na_2SO_4 at 1.23 vs. RHE. These electrodes, in conjunction with appropriate surface catalyst incorporation, are highly promising for PEC applications such as solar water splitting in appropriate PEC cell configurations.

4. Experimental

To synthesise the films, bismuth nitrate pentahydrate (7.5 mmol) was dissolved in the minimum amount of acetyl acetonate. To this was added a solution of vanadyl acetyl acetonate (7.5 mmol) in methanol, and further methanol added until 250 mL of solution was obtained. The solution was then gently heated for one hour to initiate a colour change from green to brown. Commercially available FTO (TEC 8 Pilkington, 8 Ω/sq) was used as the substrate. Substrate slides (1 cm × 2 cm) were cut by hand and ultrasonically cleansed with doubly distilled water, acetone, propan-2-ol, and then stored in ethanol. AACVD was used to fabricate the $BiVO_4$ thin films. The substrate slides were removed from the ethanol and dried in air before being transferred to the AACVD combustion chamber and heated at 500 °C for 15 min before the start of the deposition. In a typical deposition, 20 mL of the precursor was added to a round-bottomed flask placed above the piezoelectric modulator of an ultrasonic humidifier (PIFCO ultrasonic humidifier) to generate the aerosol. Air was used as the carrier gas at a flow rate of $175\,cm^3\,min^{-1}$ to transfer the aerosol into a second flask, where it was mixed with a secondary flow of air at a flow rate of $2340\,cm^3\,min^{-1}$. This drives the finer aerosol droplets towards the combustion chamber where they decompose on the heated substrate to form a $BiVO_4$ thin film. The deposition process was continued until all the 20 mL of precursor solution had been consumed.

The current-voltage (*J-V*) characteristics of the $BiVO_4$ thin films were tested using a galvanostat/potentiostat (Eco Chemie micro-Autolab type III), under illumination by an AM 1.5 class A solar simulator (Solar Light 16S–300 solar simulator), at $100\,mW\,cm^{-2}$ light intensity, calibrated by a silicon pyranometer (Solar Light Co., PMA2144 Class II). The films were measured in a three-electrode configuration in a quartz cell, using a platinum wire counter-electrode and Ag/AgCl/KCl as the reference electrode in a 1 M Na_2SO_4 electrolyte at a scan rate of $10\,mV\,s^{-1}$. The Ag/AgCl was converted to RHE by using the relation $E_{RHE} = E_{AgCl} + 0.059pH + E^{\circ}_{AgCl}$, where $E^{\circ}_{AgCl} = 0.1976$ V at 25 °C.[45]

The phase and crystallinity of the $BiVO_4$ thin films were evaluated by conducting XRD measurements using a Bruker D8 XRD, operating with monochromatic Cu Kα ($k = 1.54$ Å) radiation and Lynxeye detector. The surface morphology was studied using a Leo 1530 VP field emission gun (FEG)-SEM at an accelerating voltage of 5 kV and a working distance of 5 mm. EDX spectroscopy was also carried out in order to determine the Bi/V ratio. RS was undertaken using a HORIBA Jobin Yvon LabRAM HR (with 632.8 nm He-Ne laser) Raman spectrophotometer. The spectrum was recorded in the range $100 - 1000\,cm^{-1}$.

Received: June 23, 2014
Revised: August 29, 2014

[1] M. G. Walter, E. L. Warren, J. R. McKone, S. W. Boettcher, Q. Mi, E. A. Santori, N. S. Lewis, *Chem. Rev.* **2010**, *110*, 6446.
[2] X. Chen, S. Shen, L. Guo, S. S. Mao, *Chem. Rev.* **2010**, *110*, 6503.
[3] M. Gratzel, *Nature* **2001**, *414*, 338.
[4] S. Choudhary, S. Upadhyay, P. Kumar, N. Singh, V. R. Satsangi, R. Shrivastav, S. Dass, *Int. J. Hydrogen Energy* **2012**, *37*, 18713.
[5] S. J. Hong, S. Lee, J. S. Jang, J. S. Lee, *Energy Environ. Sci.* **2011**, *4*, 1781.
[6] Y. Park, K. J. MacDonald, K.-S. Choi, *Chem. Soc. Rev.* **2013**, *423*, 2321.
[7] S. P. Berglund, D. W. Flaherty, N. T. Hahn, A. J. Bard, C. B. Mullins, *J. Phys. Chem. C* **2011**, *115*, 3794.
[8] J. R. McKone, N. S. Lewis, H. B. Gray, *Chem. Mater.* **2014**, *26*, 407.
[9] J. A. Seabold, K.-S. Choi, *J. Am. Chem. Soc.* **2012**, *134*, 2186.
[10] F. F. Abdi, L. Han, A. H. M. Smets, M. Zeman, B. Dam, R. van de Krol, *Nat. Commun.* **2013**, *4*, 3195.
[11] P. Bornoz, F. F. Abdi, S. D. Tilley, B. Dam, R. van de Krol, M. Gratzel, K. Sivula, *J. Phys. Chem. C* **2014**, *118*, 16959.
[12] L. H. Mascaro, A. Pockett, J. M. Mitchels, L. M. Peter, P. J. Cameron, V. Celorrio, D. J. Fermin, J. S. Sagu, K. G. U. Wijayantha, G. Kociok-Kohn, F. Marken, *J. Solid State Electrochem.* **2014**, DOI: 10.1007/s10008-014-2495-y
[13] D.-D. Qin, T. Wang, Y.-M. Song, C.-L. Tao, *Dalton Trans.* **2014**, *43*, 7691.
[14] E. Alarcon-Llado, L. Chen, M. Hettick, N. Mashouf, Y. Lin, A. Javey, J. W. Ager, *Phys. Chem. Chem. Phys.* **2014**, *16*, 1651.
[15] T. W. Kim, K.-S. Choi, *Science* **2014**, *343*, 990.
[16] C. Ding, J. Shi, D. Wang, Z. Wang, N. Wang, G. Liu, F. Xiong, C. Li, *Phys. Chem. Chem. Phys.* **2013**, *15*, 4589.
[17] A. A. Tahir, T. A. N. Peiris, K. G. U. Wijayantha, *Chem. Vap. Deposition* **2012**, *18*, 107.
[18] A. A. Tahir, K. G. U. Wijayantha, M. Mazhar, V. McKee, *Thin Solid Films* **2010**, *518*, 3664.
[19] I. A. Bhatti, T. A. N. Peiris, T. D. Smith, K. G. U. Wijayantha, *Mater. Lett.* **2013**, *93*, 333.
[20] A. A. Tahir, K. G. U. Wijayantha, S. Saremi-Yarahmadi, M. Mazhar, V. McKee, *Chem. Mater.* **2009**, *21*, 3763.
[21] A. A. Tahir, H. A. Burch, K. G. U. Wijayantha, B. G. Pollet, *Int. J. Hydrogen Energy* **2013**, *38*, 4315.
[22] M. A. Ehsan, T. A. N. Peiris, K. G. U. Wijayantha, H. Khaledi, H. N. Ming, M. Misran, Z. Arifin, M. Mazhar, *Thin Solid Films* **2013**, *540*, 1.
[23] A. A. Tahir, T. D. Smith, K. G. U. Wijayantha, *Nanosci. Nanotechnol. Lett.* **2011**, *3*, 674.
[24] P. Marchand, I. A. Hassan, I. P. Parkin, C. J. Carmalt, *Dalton Trans.* **2013**, *42*, 9406.
[25] X. Hou, K.-L. Choy, *Chem. Vap. Deposition* **2006**, *12*, 583.
[26] A. A. Tahir, M. A. Ehsan, M. Mazhar, K. G. U. Wijayantha, M. Zeller, A. D. Hunter, *Chem. Mater.* **2010**, *22*, 5084.
[27] J. B. Biswal, S. S. Garje, J. Nuwad, C. G. S. Pillai, *J. Solid State Chem.* **2013**, *204*, 348.
[28] S. J. A. Moniz, D. Bachu, C. S. Blackman, A. J. Cross, S. Elouali, D. Pugh, R. Q. Cabrera, S. Vallejos, *Inorg. Chim. Acta* **2012**, *380*, 328.
[29] J. Waters, D. Crouch, J. Raftery, P. O'Brien, *Chem. Mater.* **2004**, *16*, 3289.
[30] A. Kudo, K. Omori, H. Kato, *J. Am. Chem. Soc.* **1999**, *121*, 11459.
[31] S. Tokunaga, H. Kato, A. Kudo, *Chem. Mater.* **2001**, *13*, 4624.
[32] Y. Liang, T. Tsubota, L. P. A. Mooij, R. van de Krol, *J. Phys. Chem. C* **2011**, *115*, 17594.
[33] R. L. Frost, D. A. Henry, M. L. Weier, W. Martens, *J. Raman Spectrosc.* **2006**, *37*, 722.
[34] F. D. Hardcastle, I. E. Wachs, *J. Phys. Chem.* **1991**, *95*, 5031.
[35] F. F. Abdi, T. J. Savenije, M. M. May, B. Dam, R. van de Krol, *J. Phys. Chem. Lett.* **2013**, *4*, 2752.
[36] F. F. Abdi, R. van de Krol, *J. Phys. Chem. C* **2012**, *116*, 9398.
[37] D. K. Zhong, S. Choi, D. R. Gamelin, *J. Am. Chem. Soc.* **2011**, *133*, 18370.
[38] P. Chatchai, Y. Murakami, S. Y. Kishioka, A. Y. Nosaka, Y. Nosaka, *Electrochem. Solid State Lett.* **2008**, *11*, H160.
[39] K. Sayama, A. Nomura, T. Arai, T. Sugita, R. Abe, M. Yanagida, T. Oi, Y. Iwasaki, Y. Abe, H. Sugihara, *J. Phys. Chem. B* **2006**, *110*, 11352.
[40] M. T. McDowell, M. F. Lichterman, J. M. Spurgeon, S. Hu, I. D. Sharp, B. S. Brunschwig, N. S. Lewis, *J. Phys. Chem. C* **2014**, *118*, 19618.
[41] Y. Zhang, J. Wang, Y. Zhao, J. Zhai, L. Jiang, Y. Song, D. J. Zhu, *J. Mater. Chem.* **2008**, *18*, 2650.
[42] Q. Jia, K. Iwashina, A. Kudo, *Proc Natl Acad Sci USA* **2012**, *109*, 11564.
[43] A. J. E. Rettie, H. C. Lee, L. G. Marshall, J.-F. Lin, C. Capan, J. Lindemuth, J. S. McCloy, J. Zhou, A. J. Bard, C. B. Mullins, *J. Am. Chem. Soc.* **2013**, *135*, 11389.
[44] M. F. Lichterman, M. R. Shaner, S. G. Handler, B. Brunschwig, H. B. Gray, N. S. Lewis, J. M. Spurgeon, *J. Phys. Chem. Lett.* **2013**, *4*, 4188.
[45] A. Kay, I. Cesar, M. Gratzel, *J. Am. Chem. Soc.* **2006**, *128*, 15714.

